

ELECTRON CLOUD EFFECTS

G. Iadarola* and G. Rumolo
CERN, Geneva, Switzerland

Abstract

Secondary electron emission in combination with the electromagnetic fields generated by a bunched beam can lead to the formation of electron clouds in the beam chambers of particle accelerators. The interaction of the circulating beam with the e-cloud can lead to transverse instabilities, beam losses, transverse emittance degradation. Moreover, the electrons impacting on the chamber's walls induce other unwanted effects like energy deposition (particularly critical for superconducting machines) and vacuum degradation. This contribution summarizes the mechanisms leading to the formation of the e-cloud, the effects that it can have on the performance of an accelerator, the methods employed to study the phenomenon and different techniques that have been developed to reduce or suppress its formation.

INTRODUCTION

Over the last five decades electron cloud effects have been observed in several circular accelerators operating with positively charged particles [1, 2]. A synthesis of the main observation in different machines is given Tab. 1.

The mechanism leading to the formation of an e-cloud in the beam chamber of a particle accelerator is illustrated schematically in Fig. 1 [3, 4]. "Primary" or "seed" electrons can be generated by a bunch passage due to the ionization of the residual gas or to photo-emission from the chamber's wall induced by the beam synchrotron radiation. These electrons can be accelerated by the electric field of the beam, typically to energies in the order of hundreds of electronvolts. When an electron with these energies impacts on the walls, secondary electron emission can occur and multiple low-energy electrons can be emitted. These "secondary electrons" have lower kinetic energy (~ 10 eV). In case they impact the wall, there is a high probability of them being absorbed without generating any further secondary. However, if the delay between subsequent bunches (bunch spacing) is sufficiently short, before impacting on the wall they can be accelerated by the following bunch passage, which strongly increases their probability of generating more secondaries. For a long bunch train, this can lead to an avalanche electron multiplication and to the formation of a dense e-cloud in the chamber (this regime is often called beam-induced "multipacting"). This mechanism makes the electron density larger for the bunches at the tail of bunch trains.

The e-cloud can induce unwanted effects on the circulating beam such as transverse instabilities, transverse emittance blow-up and particle losses. Other unwanted effects are vacuum degradation due to electron-stimulated desorption

and power deposition (heat loads) on the chamber's walls (particularly critical for superconducting devices) [5].

MAIN FACTORS INFLUENCING THE ELECTRON CLOUD FORMATION

Observing the sketch in Fig. 1, it is possible to identify different factors that influence the e-cloud buildup process.

A very important role is played by the beam chamber. Its geometry affects the electron acceleration and time-of-flight between impacts. It also defines the boundary conditions for the calculation of the electric field generated by the beam and by the electrons themselves. Moreover the chamber surface properties will define the amount of electrons generated by photoemission and, most importantly, the probability of secondary emission occurring when an electron impacts on the wall [6, 7].

The secondary emission process is described by the Secondary Electron Yield (SEY) function, which is defined as the ratio between the impinging electron current and the emitted electron current and depends strongly on the energy of the impinging electrons (the SEY is often indicated with the symbol " δ "). Typical SEY curves are shown in Fig. 2. A synthetic parameter which is often used to describe the surface is the maximum of the SEY curve (indicated as SEY_{max} or δ_{max}). The dependence of the SEY on the energy of the impacting electrons is typically non-monotonic. As a result, there will be a defined energy range, indicated in red in Fig. 2, for which $\delta(E) > 1$ and the surface globally behaves like an electron emitter. For the e-cloud buildup to occur it is necessary to have a significant fraction of the impacting electrons with energies within this range. The SEY is also dependent on the angle of incidence of the electrons and, in particular, it tends to be higher for grazing angles.

The SEY depends on the chemical properties of the surface and can be affected by different processes. In particular, for several materials, the SEY decreases when the surface is exposed to an electron flux [8]. For this reason the e-cloud is, to some extent, a "self-healing" mechanism in the sense that the surface can be conditioned by exposing it to the e-cloud itself (this effect is called "beam-induced scrubbing").

The beam configuration also plays a major role in the e-cloud buildup process. As observed before a key parameter is the bunch spacing, which determines the amount of electrons surviving between consecutive bunch passages. In particular, the bunch spacing strongly affects the "multipacting threshold", defined as the value of δ_{max} above which the avalanche multiplication occurs. An example is shown in Fig. 3 for the case of a bending magnet of the Large Hadron Collider (LHC). In this case, with the 25 ns bunch spacing, multipacting occurs for δ_{max} values larger than 1.4 while with the 50 ns bunch spacing the e-cloud buildup only takes

* Giovanni.Iadarola@cern.ch

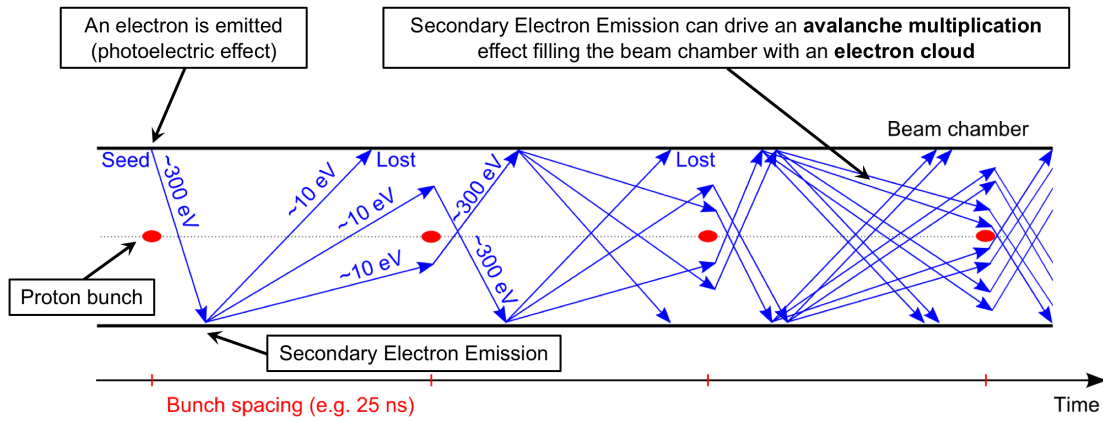


Figure 1: Schematic illustration of the e-cloud buildup process.

Year	Place	Observations
1965	Novosibirsk, Argonne ZGS, BNL AGS	Transverse instabilities.
1970s	CERN ISR, Bevatron	Transverse instabilities, vacuum degradation.
1988	Los Alamos PSR	Transverse instabilities.
1989	KEK PF	Multibunch instability for positron bunch trains
1999	CERN SPS and PS, KEKB and PEP-II	Pressure rise, transverse instabilities, effects on instrumentation, tune shifts along bunch train, emittance degradation.
2002	RHIC	Pressure rise, tune shift, transverse instabilities at transition.
2003-2009	Tevatron, SNS, DaΦne, ANKA, PETRA III, J-PARC main ring	Vacuum degradation, transverse instabilities, transverse blow-up, heat load on cryogenic devices.
2008-present	Cesr-TA	A program to study electron cloud issues is conducted.
2010-present	LHC	Vacuum degradation, transverse instabilities, beam degradation, heat loads in cryogenic devices.
2014	FERMILAB recycler	Transverse instabilities.
2016-present	SuperKEKB	Dynamic pressure rise, beam degradation.

Table 1: Summary of the main observations of e-cloud effects in particle accelerators (largely based on [1]).

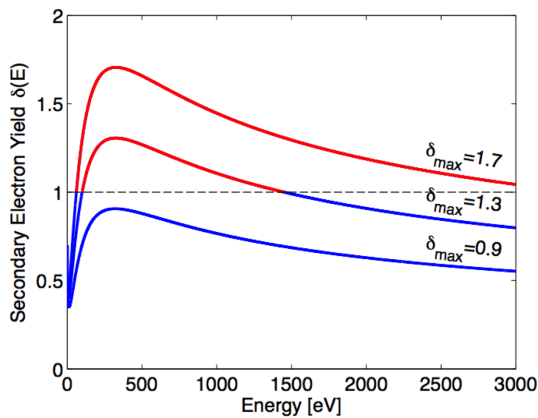


Figure 2: Examples of SEY curves for different values of the δ_{max} parameter.

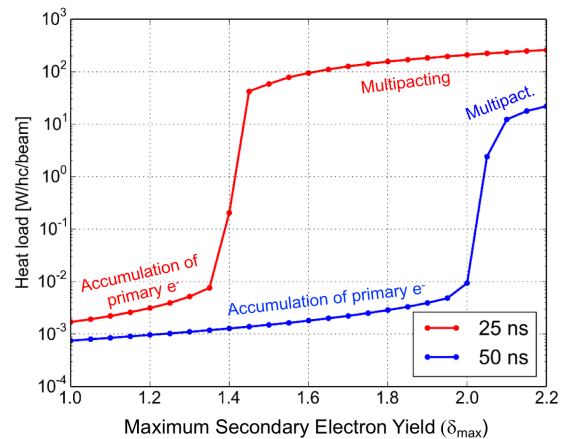


Figure 3: Heat load in the LHC bending magnet for 25 ns and 50 ns bunch spacing (PyECLLOUD simulations).

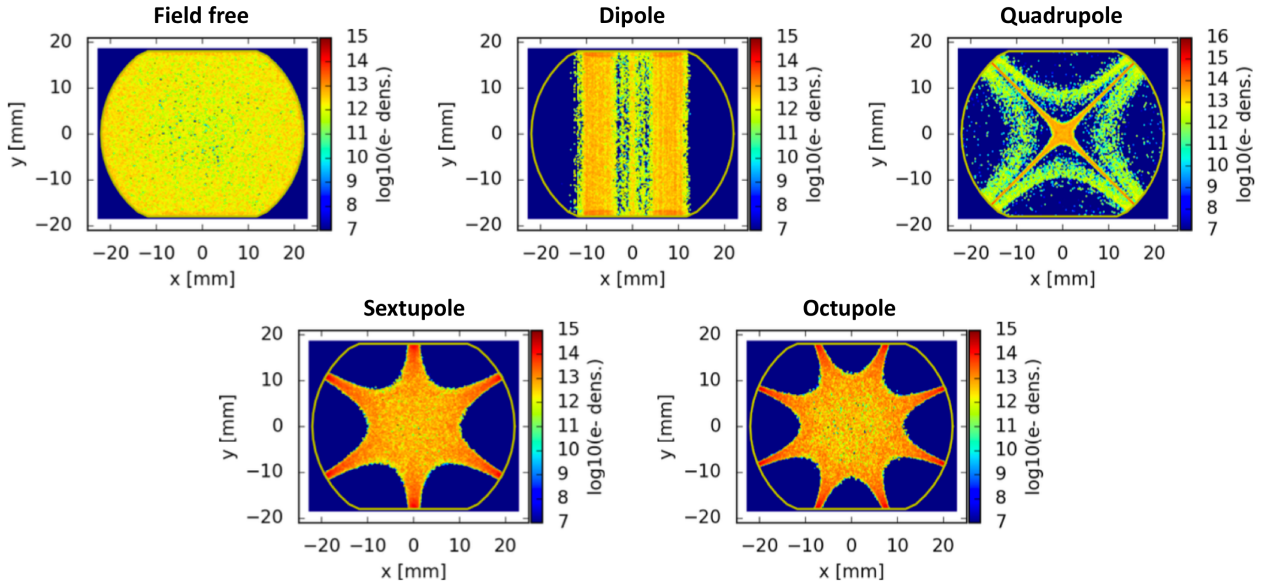


Figure 4: Electron distribution in LHC arc components with different magnetic field configurations (PyECLLOUD simulations).

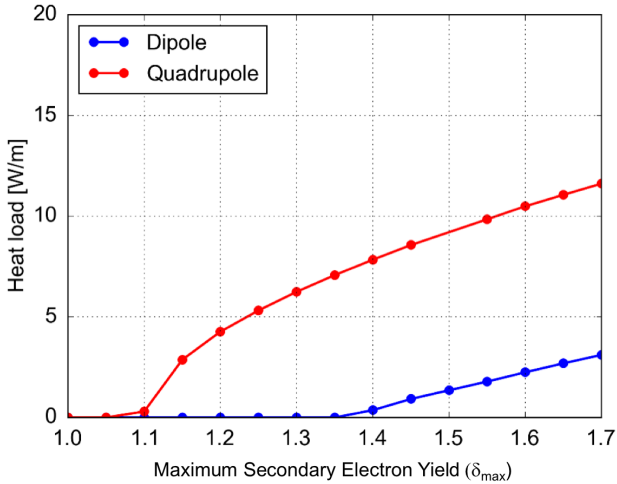


Figure 5: Heat loads generated by e-cloud the LHC dipole and quadrupole magnets (PyECLLOUD simulations for 25 ns bunch spacing).

place for $\delta_{max} > 2.0$. Other beam parameters such as bunch intensity and bunch length also influence the e-cloud dynamics, as they change the acceleration received by the electrons from the beam.

Due to the very low kinetic energy, the electron trajectories are strongly influenced by externally applied magnetic fields. For large enough magnetic fields, the electrons spin around the field lines. This effect, together with the shape of the SEY curve and the beam electric field, determines very characteristic patterns in the distribution of the electrons within the beam chamber as shown in Fig. 4.

In quadrupole magnets and higher order multipoles, due to the presence of magnetic field gradients, magnetic trapping

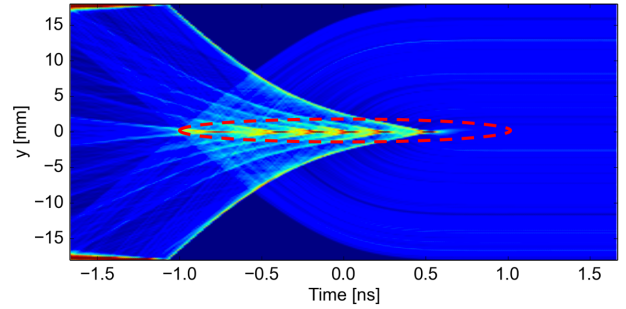


Figure 6: Electron cloud density evolution in the horizontal plane of a bending magnet during the passage of a bunch (PyECLLOUD simulation).

can occur [9]. Electrons can survive several bunch passages and accumulate energy from more than one bunch, reaching energies up to a few kiloelectronvolts. In the case of the LHC quadrupoles this results in heat loads that are much stronger compared to the dipole magnets, as shown in Fig. 5 [10].

EFFECT OF THE ELECTRON CLOUD ON THE BEAM DYNAMICS

When a bunch of positively charged particle travels in an e-cloud, electrons are attracted towards the bunch and “fly” through it, exerting significant electromagnetic forces on the beam particles. In particular, the electron density at the beam location increases during the bunch passage (“pinch” effect) as illustrated in Fig. 6. As a consequence of this dynamics, several effects on the circulating beam can be observed.

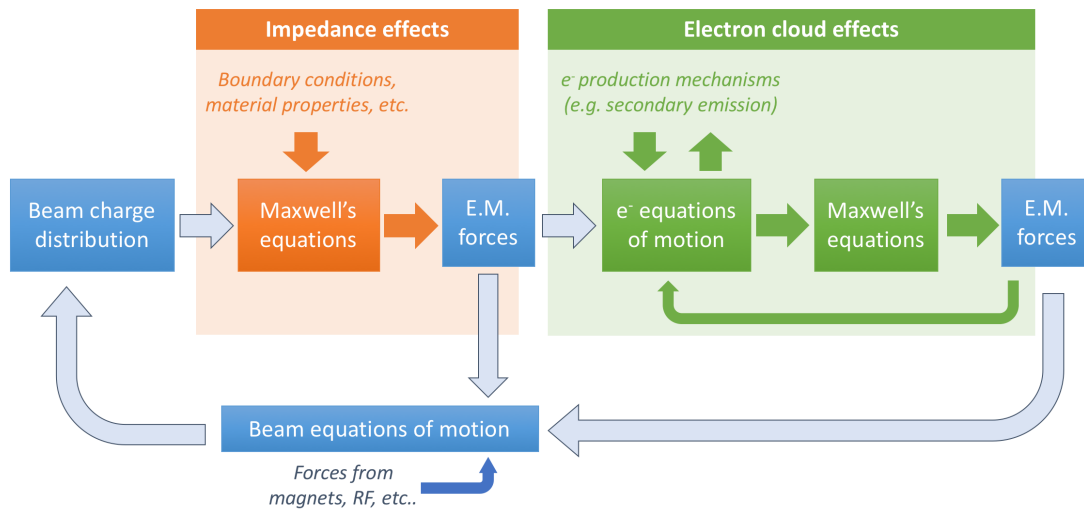


Figure 7: Block diagram illustrating the mechanism of beam instabilities driven by e-cloud.

Instabilities

The interaction of the beam with the e-cloud can generate transverse instabilities [11–13]. A block diagram of the coupled dynamics of the beam and the e-cloud is shown in Fig. 7. The orange box represents conventional impedance effects: the beam charge distribution generates electromagnetic fields in the beam chambers, which enter as a driving term in the beam equation of motion, causing modifications in the beam distribution. In this case the relation between the beam distribution and the resulting forces on the beam is linear and time-invariant. It can therefore be described by its pulse response (wakefield) and the effect on a generic distribution can be obtained using the linear superposition (convolution integral). In the presence of electrons in the chamber, the electromagnetic forces of the beam will also participate in the electrons' equation of motion and possibly drive the electron multipacting. The electron cloud in turn generates electromagnetic forces, which act back on the beam. The fast motion of the electrons, makes the response of the “e-cloud system” (green box in Fig. 7) neither linear nor time invariant. Therefore the wakefield formalism cannot be used for the description of these phenomena.

The interaction with the e-cloud introduces an additional closed loop in the diagram in Fig. 7, which can amplify the beam oscillations triggering a transverse instability. An e-cloud can drive both coupled-bunch and single-bunch instabilities.

Coupled-bunch instabilities driven by e-cloud have been observed in several machines (e.g. CERN PS and SPS, KEKB, FERMILAB Recycler). Bunches at the tail of the trains are the most affected as they encounter a larger electron density. These instabilities result from alterations of the e-cloud buildup due to transverse oscillations of the beam. They have been successfully modeled analytically using a simple cloud-bunch coupling relation [14, 15]. Typically these instabilities can be effectively controlled with conventional (bunch-by-bunch) transverse feedback systems.

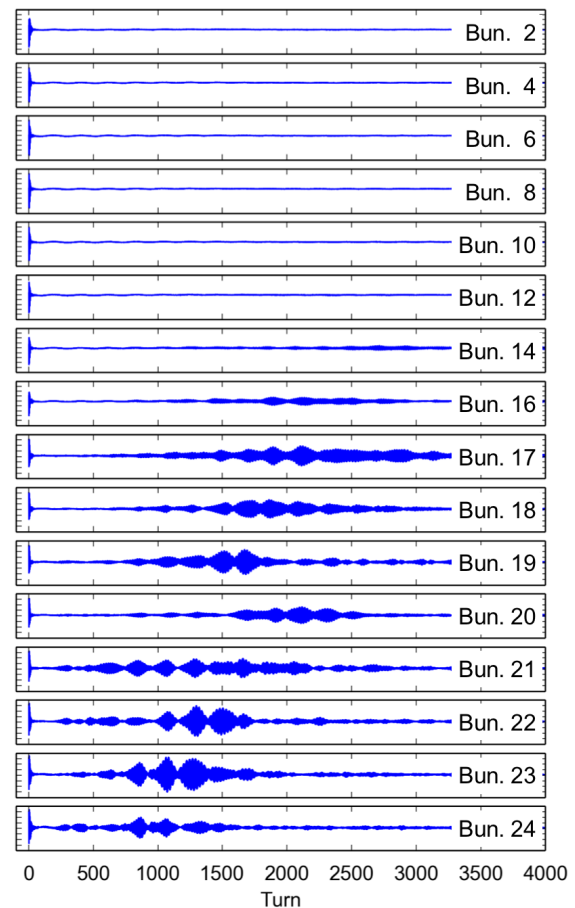


Figure 8: Position measurements for different bunches in a train right after its injection into the LHC. Transverse instabilities can be observed at the tail of the bunch train.

Single bunch instabilities are driven by the motion of the electrons during an individual bunch passage (electron pinch). Typically groups of bunches at the tail of the bunch trains are simultaneously affected but no correlation is ob-

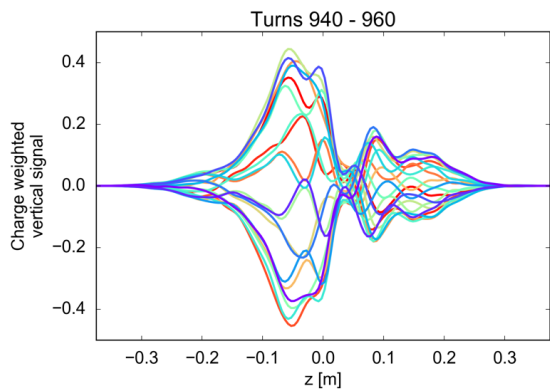


Figure 9: Slice-by-slice position centroid (charge weighted) along an LHC bunch undergoing an e-cloud instability. The different traces correspond to 20 consecutive turns (PyECLOUD-PyHEADTAIL simulation).

served in the centroid motion of the different bunches (an example is shown in Fig. 8). These instabilities can develop very rapidly (with rise-times in the order of $10^2 - 10^3$ turns) and result in beam losses and strong transverse emittance blow-up. As electrons move very fast during the bunch passage, single bunch instabilities driven by e-cloud are characterized by a fast intra-bunch motion, as shown in Fig. 9. For this reason, these instabilities cannot be damped effectively with conventional transverse feedback systems. However, they can be mitigated to some extent operating with large chromaticity and/or with strong amplitude detuning introduced by octupole magnets [16], often at expense of the achievable beam lifetime and emittance preservation. Efforts are ongoing for the development of high-bandwidth feedback systems capable of damping the observed intra-bunch motion [17].

Other effects on the beam

Even when electron densities are low enough not to trigger instabilities, the effect of the e-cloud is still visible on several beam properties.

The presence of the electrons introduces extra focusing forces which in most cases result in a positive shift of the coherent betatron tune, increasing along the bunch train (an example is shown in Fig. 10) [18].

When electrons are accelerated by a bunch passage, energy is transferred from the beam to the electron cloud. In a synchrotron, this results in a shift of the bunch stable phase with respect to the RF system [19]. Tune shift and stable phase measurements are often used as indirect e-cloud diagnostics.

The forces exerted by the e-cloud on the beam particles depend non-linearly on the particle's positions. This can excite resonant lines in the tune diagram and induce quite large tune spreads, especially in combination with octupoles and chromaticity settings that are required to protect the beam from e-cloud instabilities. This results in slow particle losses, emittance growth and bunch shortening (loss of par-

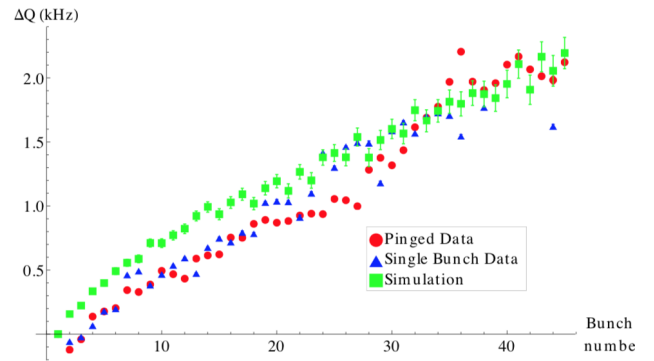


Figure 10: Simulated and measured tune shift for different bunches of a bunch train in the CESR-TA ring (from [18]).

ticles having large longitudinal amplitude). Figure 11 shows the tune footprint estimated for one of the last bunches of an LHC train at injection energy (450 GeV). The asymmetry of the footprint with respect to the unperturbed tune (black star) is introduced by the e-cloud. In order to avoid beam losses due to the interaction with the resonance $Q_v = .33$ it was necessary to change the machine tune settings as shown in Fig. 11 [20].

OTHER EFFECTS ON MACHINE PERFORMANCE

Together with the aforementioned unwanted effects on the beam, the e-cloud can pose other limitations to the operation of an accelerator.

Electrons impacting on the walls of the beam pipe can deposit a significant power on the chamber walls. Looking at the illustration in Fig. 1 one can see that only a small fraction of the energy of the impinging electrons is carried by the secondary electrons, while a much larger fraction is dissipated in the walls. This aspect is particularly critical for superconducting machines, where the cooling capacity on the beam chamber is very limited. In the LHC beam screens are installed, which are operated at temperatures higher than the superconducting coils, in order to ease the extraction of beam induced heat loads [21]. When operating with nominal bunch spacing (25 ns) e-clouds develop in the superconducting arc magnets generating heat loads that are much higher than observed with larger bunch spacings (a comparison between 25 ns and 50 ns is shown in Fig. 12) [22]. In order to operate reliably with the 25 ns bunch spacing a dedicated feed-forward control had to be developed in order to dynamically adapt the cryogenic regulations using the measured properties of the circulating beam, based on pre-computed e-cloud models [23].

The flux of electrons impinging on the walls also generates vacuum degradation due to electron-stimulated desorption [24]. This can pose different problems, for example increased background in collider experimental regions and

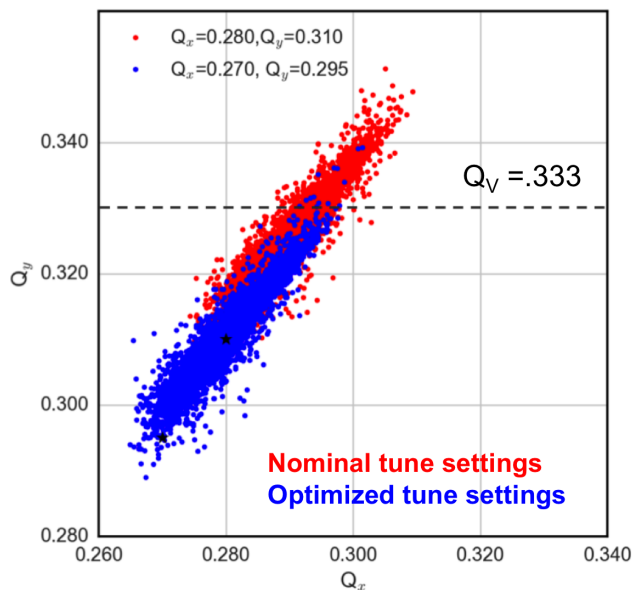


Figure 11: Tune footprints evaluated for a LHC bunch at injection including the effect of octupoles powered at 26 A, $Q'_{x,y}$ at 15 units, and EC in dipole and quadrupole magnets. The dashed line represents the third order resonance $Q_y = .33$. The black star represents the unperturbed tune for the optimized settings.

risk of breakdown in high voltage devices like kickers or electrostatic septa.

The presence of e-cloud can also induce malfunctions on beam diagnostic devices [25].

NUMERICAL MODELING

The understanding of e-cloud phenomena heavily relies on MacroParticle (MP) simulations. The full modeling of the coupled dynamics of the beam and the e-cloud is computationally very heavy, as it involves multiple space and time scales. In particular one needs to simulate the electron dynamics over the entire beam chamber ($\sim 1 - 10$ cm wide) while having enough spacial resolution within the beam transverse size ($\sim 0.1 - 1$ mm). Moreover, while the electron motion happens at the 1 ns time-scale, the effects on the beam stability are visible only when the action of the e-cloud is accumulated over many turns (the typical instability rise-times are in the range $\sim 1 - 10$ s).

Fully self-consistent simulations have been made only rarely and require considerable computing resources ($\sim 10^3$ CPUs) [26]. More often the problem is studied in two stages [27, 28]:

1. e-cloud “build-up simulations” employ Particle-In-Cell (PIC) methods to study exclusively the dynamics of the electrons and the multipacting process using an unperturbed beam distribution. Examples of buildup codes are CLOUDLAND, E-CLOUD and its evolution PyE-CLOUD, PEI, POSINST.

2. “Beam-dynamics simulations” study the interaction of the beam (typically a single bunch) with a given initial electron distribution obtained from a buildup simulation. Even with these simplifications, the more demanding cases (e.g. LHC at high energy) can be computationally very demanding, requiring advanced computational techniques (e.g. multi-grid Poisson solvers) and the usage of parallel computing resources. Examples of this kind of simulation codes are CMAD, HEAD-TAIL and its evolution PyE-CLOUD-PyHEADTAIL, PEHTS.

MITIGATION TECHNIQUES

Several techniques have been developed to mitigate the electron cloud formation, which can be grouped in two categories:

- Techniques relying on modifications of the surface behavior. The most widely used are:
 - Beam induced conditioning or “scrubbing” consists in operating the accelerator with beam configurations that enhance the e-cloud production. For several materials, the exposition of the surface to the electron flux decreases the SEY mitigating the e-cloud [29];
 - Morphological changes of the surface: the SEY can be reduced by increasing the surface roughness (using for example laser ablation), or introducing macroscopic grooves [30–32];
 - Coating of the surface with materials which have intrinsically low SEY (e.g. amorphous carbon, TiN, NEG) [33].
- Techniques acting on the electron dynamics. They aim in particular at decreasing the probability of electrons surviving between consecutive bunch passages:
 - Electric fields can be applied in the beam chambers using so called “clearing electrodes” to push secondary electrons back on the surface [34];
 - Weak longitudinal magnetic fields can be applied using solenoids or permanent magnets to bend the secondary electron trajectories back on the surface [35, 36].

These techniques are included in the designs for several ongoing and future projects like SuperKEKB, High Luminosity LHC and the design study for Future Circular Colliders (FCC).

ACKNOWLEDGMENTS

The authors would like to thank G. Arduini, P. Dijkstal, K. Li, L. Mether, E. Metral, A. Romano, G. Skripka for their important input to the present contribution.

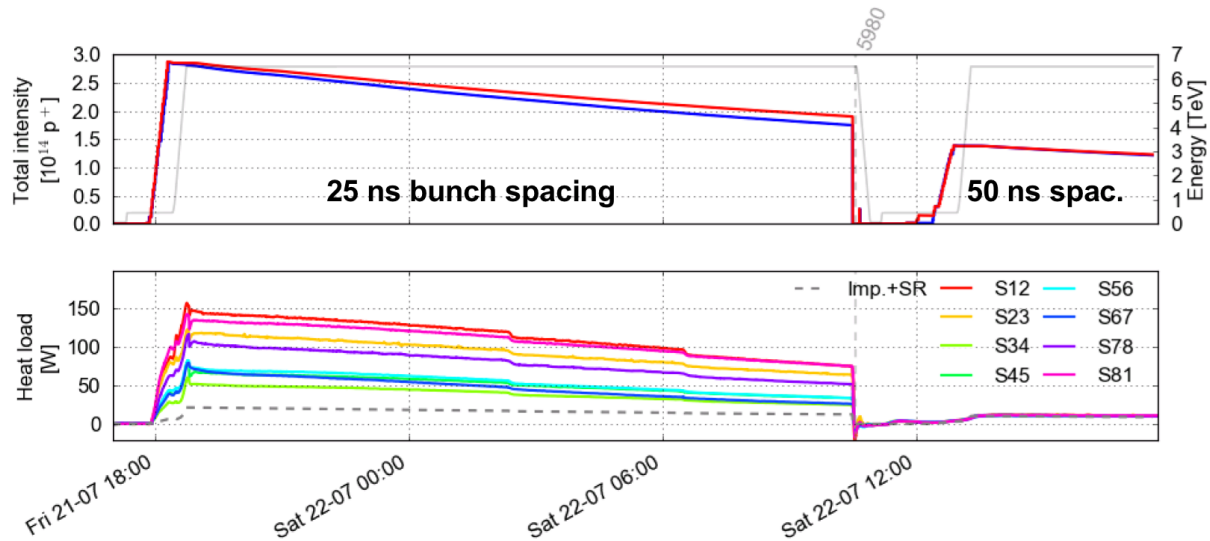


Figure 12: Average heat loads measured in the half-cells of the LHC arcs with two different bunch spacings [22].

REFERENCES

- [1] F. Zimmermann, “Electron-Cloud Effects in past and future machines - walk through 50 years of Electron-Cloud studies,” in *Proceedings, 5th Workshop on Electron-Cloud Effects (E-CLOUD’12): La Biodola, Isola d’Elba, Italy, June 5-9, 2012*, 2013.
- [2] R. Cimino and T. Demma, “Electron cloud in accelerators,” *International Journal of Modern Physics A*, vol. 29, no. 17, p. 1430023, 2014.
- [3] M. A. Furman, “Formation and dissipation of the electron cloud,” in *Proceedings of the 2003 Particle Accelerator Conference*, vol. 1, pp. 297–302 Vol.1, May 2003.
- [4] G. Iadarola, “Electron cloud studies for CERN particle accelerators and simulation code development.” CERN-THESIS-2014-047, 2014.
- [5] G. Rumolo, F. Ruggiero, and F. Zimmermann, “Simulation of the electron-cloud build up and its consequences on heat load, beam stability, and diagnostics,” *Physical Review Special Topics-Accelerators and Beams*, vol. 4, no. 1, p. 012801, 2001.
- [6] M. A. Furman and M. T. F. Pivi, “Probabilistic model for the simulation of secondary electron emission,” *Phys. Rev. ST Accel. Beams*, vol. 5, p. 124404, Dec 2002.
- [7] R. Cimino, I. R. Collins, M. A. Furman, M. Pivi, F. Ruggiero, G. Rumolo, and F. Zimmermann, “Can low-energy electrons affect high-energy physics accelerators?,” *Phys. Rev. Lett.*, vol. 93, p. 014801, Jun 2004.
- [8] F. Le Pimpec, R. E. Kirby, F. K. King, and M. Pivi, “Electron conditioning of technical aluminium surfaces: Effect on the secondary electron yield,” *Journal of Vacuum Science & Technology A*, vol. 23, no. 6, pp. 1610–1618, 2005.
- [9] M. G. Billing, J. Conway, E. E. Cowan, J. A. Crittenden, W. Hartung, J. Lanzoni, Y. Li, C. S. Shill, J. P. Sikora, and K. G. Sonnad, “Measurement of electron trapping in the cornell electron storage ring,” *Phys. Rev. ST Accel. Beams*, vol. 18, p. 041001, Apr 2015.
- [10] P. Dijkstal, G. Iadarola, L. Mether, and G. Rumolo, “Simulation studies on the electron cloud build-up in the elements of the LHC Arcs at 6.5 TeV,” *CERN-ACC-NOTE-2017-0057*, Oct 2017.
- [11] K. Ohmi and F. Zimmermann, “Head-tail instability caused by electron clouds in positron storage rings,” *Phys. Rev. Lett.*, vol. 85, pp. 3821–3824, Oct 2000.
- [12] G. Rumolo and F. Zimmermann, “Electron cloud simulations: beam instabilities and wakefields,” *Phys. Rev. ST Accel. Beams*, vol. 5, p. 121002, Dec 2002.
- [13] A. Romano, O. Boine-Frankenheim, X. Buffat, G. Iadarola, and G. Rumolo, “Electron cloud buildup driving spontaneous vertical instabilities of stored beams in the large hadron collider,” *Phys. Rev. Accel. Beams*, vol. 21, p. 061002, Jun 2018.
- [14] G. Arduini, T. Bohl, K. Cornelis, W. Höfle, E. Métral, and F. Zimmermann, “Beam observations with electron cloud in the CERN PS and SPS complex,” *CERN-2005-001*, 2005.
- [15] S. A. Antipov, P. Adamson, A. Burov, S. Nagaitsev, and M.-J. Yang, “Fast instability caused by electron cloud in combined function magnets,” *Phys. Rev. Accel. Beams*, vol. 20, p. 044401, Apr 2017.
- [16] K. S. B. Li and G. Rumolo, “Mitigation of Electron Cloud Instabilities in the LHC Using Sextupoles and Octupoles,” *Conf. Proc.*, vol. C1205201, pp. 3084–3086, 2012.
- [17] J. M. Cesaratto, J. D. Fox, C. H. Rivetta, D. Alesini, A. Drago, A. Gallo, F. Marcellini, M. Zobov, S. De Santis, Z. Paret, A. Ratti, H. Qian, H. Bartosik, W. Hofle, and C. Zannini, “SPS Wideband Transverse Feedback Kicker: Design Report,” *CERN-ACC-NOTE-2013-0047*, Dec 2013.
- [18] M. G. Billing, G. Dugan, M. J. Foster, D. L. Kreinick, R. E. Meller, M. A. Palmer, G. A. Ramirez, N. T. Rider, M. Rendina, K. Sonnad, J. P. Sikora, H. A. Williams, R. L. Holtzapple, J. Y. Chu, and J. W. Flannagan, “Status of electron cloud dynamics measurements at CESR,” in *Proceedings, 2nd International Conference, IPAC 2011, San Sebastian, Spain, September 4-9, 2011*, p. MOPS084, 2011.

- [19] J. F. Esteban Müller, P. Baudrenghien, T. Mastoridis, E. Shaposhnikova, and D. Valuch, “High-accuracy diagnostic tool for electron cloud observation in the LHC based on synchronous phase measurements,” *Phys. Rev. ST Accel. Beams*, vol. 18, p. 112801, Nov 2015.
- [20] A. Romano, G. Iadarola, K. Li, and G. Rumolo, “Macroparticle Simulation Studies of the LHC Beam Dynamics in the Presence of Electron Cloud,” in *Proceedings, 8th International Conference, IPAC 2017, Copenhagen, Denmark, May 14-19, 2017*, p. TUPVA018, 2017.
- [21] E. Hatchadourian, P. Lebrun, and L. Taviani, “Supercritical Helium Cooling of the LHC Beam Screens,” *LHC-Project-Report-212*, p. 5 p, Jul 1998.
- [22] G. Iadarola, G. Rumolo, P. Dijkstal, and L. Mether, “Analysis of the beam induced heat loads on the LHC arc beam screens during Run 2,” *CERN-ACC-NOTE-2017-0066*, Dec 2017.
- [23] B. Bradu, A. Tovar González, E. Blanco Viñuela, P. Plutecki, E. Rogez, G. Iadarola, G. Ferlin, and B. Fernández Adiego, “Compensation of beam induced effects in LHC cryogenic systems,” in *Proc. of International Particle Accelerator Conference (IPAC’16), Busan, Korea, May 8-13, 2016*, 2016.
- [24] S. Y. Zhang, M. Bai, M. Blaskiewicz, P. Cameron, A. Drees, W. Fischer, D. Gassner, J. Gullotta, P. He, H. C. Hseuh, H. Huang, U. Iriso-Ariz, R. Lee, W. W. Mackay, B. Oerter, V. Ptitsyn, V. Ponnaiyan, T. Roser, T. Satogata, L. Smart, D. Trbojevic, and K. Zeno, “Rhic pressure rise and electron cloud,” in *Proceedings of the 2003 Particle Accelerator Conference*, vol. 1, pp. 54–56 Vol.1, May 2003.
- [25] W. Höfle, “Observations of the electron cloud effect on pick-up signals in the SPS,” *CERN-SL-2000-007-DI*, 2000.
- [26] M. A. Furman, J. L. Vay, and M. Venturini, “Direct Numerical Modeling of E-Cloud Driven Instability of Three Consecutive Batches in the CERN SPS,” *Conf. Proc.*, vol. C1205201, pp. 1125–1127, 2012.
- [27] E. Benedetto *et al.*, “Review and comparison of simulation codes modeling electron-cloud build up and instabilities,” in *9th European Particle Accelerator Conference (EPAC 2004) Lucerne, Switzerland, July 5-9, 2004*, 2004.
- [28] G. Iadarola, E. Belli, K. Li, L. Mether, A. Romano, and G. Rumolo, “Evolution of Python Tools for the Simulation of Electron Cloud Effects,” in *Proceedings, 8th International Particle Accelerator Conference (IPAC 2017): Copenhagen, Denmark, May 14-19, 2017*, p. THPAB043, 2017.
- [29] G. Iadarola, B. Bradu, P. Dijkstal, L. Mether, and G. Rumolo, “Impact and Mitigation of Electron Cloud Effects in the Operation of the Large Hadron Collider,” in *Proceedings, 8th International Particle Accelerator Conference (IPAC 2017): Copenhagen, Denmark, May 14-19, 2017*, p. TUPVA019, 2017.
- [30] G. Tang, A. C. Hourd, and A. Abdolvand, “Nanosecond pulsed laser blackening of copper,” *Applied Physics Letters*, vol. 101, no. 23, p. 231902, 2012.
- [31] R. Valizadeh, O. B. Malyshev, S. Wang, S. A. Zolotovskaya, W. Allan Gillespie, and A. Abdolvand, “Low secondary electron yield engineered surface for electron cloud mitigation,” *Applied Physics Letters*, vol. 105, no. 23, p. 231605, 2014.
- [32] R. Valizadeh, O. B. Malyshev, S. Wang, S. A. Zolotovskaya, A. W. Gillespie, and A. Abdolvand, “Low Secondary Electron Yield Engineered Surface for Electron Cloud Mitigation,” *Appl. Phys. Lett.*, vol. 105, p. 231605, 2014.
- [33] P. C. Pinto, S. Calatroni, H. Neupert, D. Letant-Delrieux, P. Edwards, P. Chiggiato, M. Taborelli, W. Vollenberg, C. Yin-Vallgren, J. Colaux, and S. Lucas, “Carbon coatings with low secondary electron yield,” *Vacuum*, vol. 98, pp. 29 – 36, 2013. 14th Joint Vacuum Conference/12th European Vacuum Conference/11th Annual Meeting of the Deutsche Vakuum Gesellschaft/ 19th Croatian-Slovenian Vacuum Meeting, 04-08 June 2012, Dubrovnik, Croatia.
- [34] Y. Suetsugu, H. Fukuma, L. Wang, M. Pivi, A. Morishige, Y. Suzuki, M. Tsukamoto, and M. Tsuchiya, “Demonstration of electron clearing effect by means of a clearing electrode in high-intensity positron ring,” *Nuclear Instruments and Methods in Physics Research Section A: Accelerators, Spectrometers, Detectors and Associated Equipment*, vol. 598, no. 2, pp. 372 – 378, 2009.
- [35] H. Fukuma, J. Flanagan, K. Hosoyama, T. Ieiri, T. Kawamoto, T. Kubo, M. Suetake, S. Uno, S. S. Win, and M. Yoshioka, “Status of solenoid system to suppress the electron cloud effects at the kekb,” *AIP Conference Proceedings*, vol. 642, no. 1, pp. 357–359, 2002.
- [36] Y. Suetsugu, K. Shibata, T. Ishibashi, K. Kanazawa, M. Shirai, S. Terui, and H. Hisamatsu, “First commissioning of the superkekb vacuum system,” *Phys. Rev. Accel. Beams*, vol. 19, p. 121001, Dec 2016.